

11) J. Davies, et. al., "GMTIFS: The Adaptive Optics Beam Steering Mirror for the GMT Integral-Field Spectrograph", Proc SPIE, 9912, 991217 (2016)

The aim of these tests was to demonstrate that a guide star can be acquired and reacquired to the  $1\ \mu\text{m}$  specification, irrespective of attitude. The test utilizes the BSM flexure rig to mount a point source microscope (PSM) on axis with the BSM, where the PSM provides a representative guide star at the nominal focal plane. The test configuration shown in Figure 3, below, displays the flexure test rig. The BSM assembly is interfaced to the controller rack that includes the PIE-712 piezo controller; the Kaman DIT-5200 and SMT-9700 eddy current sensor systems; and the Attocube FPS3010 interferometer system. The PSM and inertial system (INS) are controlled by their respective software applications on a separate laptop.

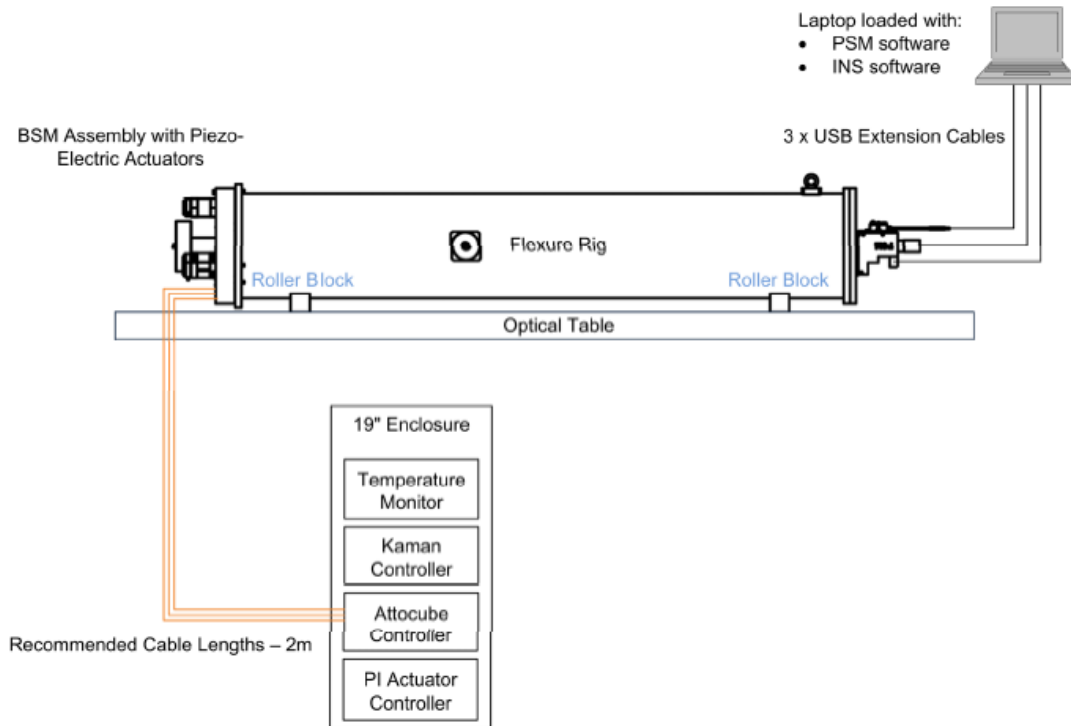


Figure 3. Overview of Axial Mechanism Flexure Configuration

12) A. Sheinis, et. al., "First light results from the high efficiency and resolution multi-element spectrograph at the Anglo-Australian telescope", *Journal of Astronomical Telescopes, Instruments, and Systems*, 1(3), 035002

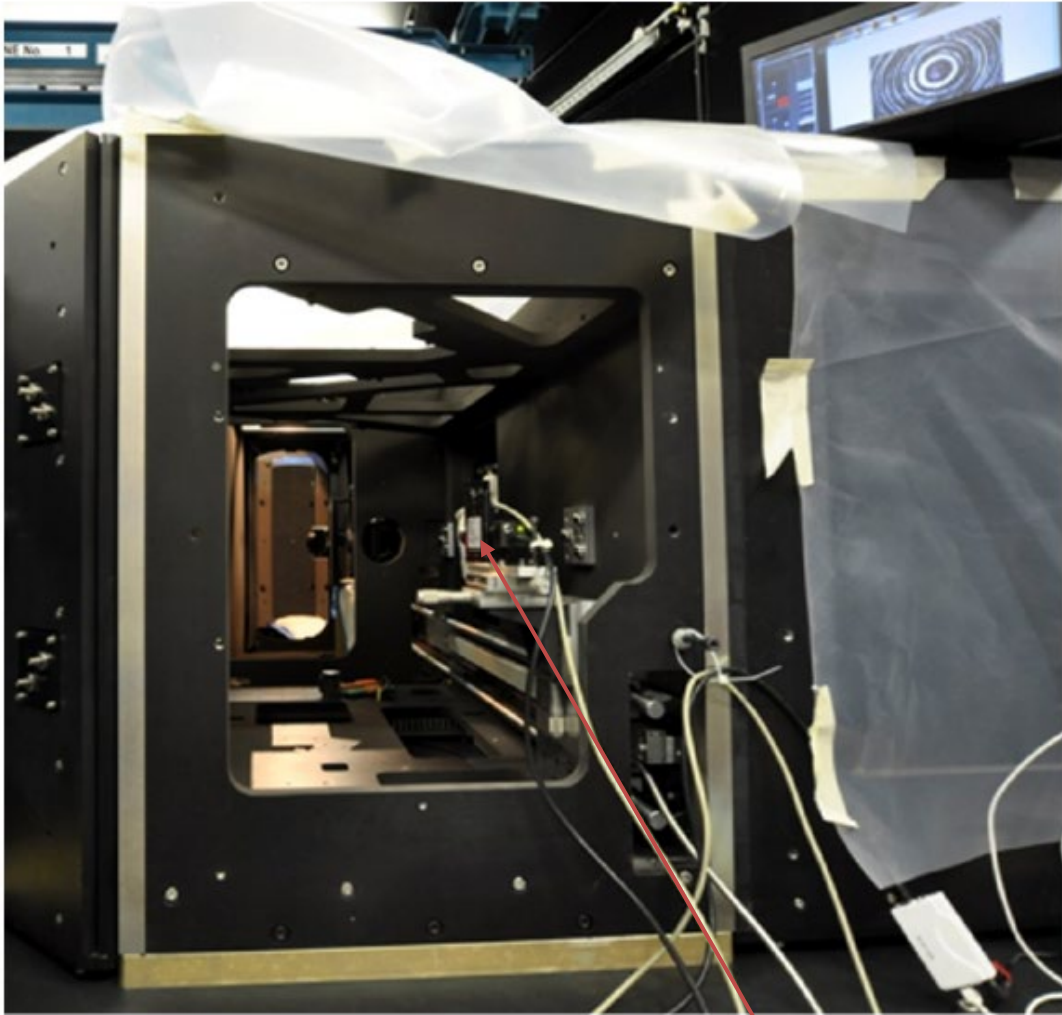


Figure 12: View looking down central spine during collimator alignment. PSM mounted on linear rail.

14) L. Gers and N. Staszak, "Deterministic optical alignment of HERMES", Proc SPIE, 9151, 915113 (2014)

The optical alignment of HERMES used a variety of precision alignment tools that can be purchased off the shelf including the Point Source Microscope (PSM) from Optical Perspectives, the Alignment Pip Generator from Jenoptik Optical Systems, and an autocollimating alignment telescope from Davidson Optronics. HERMES also used a significant amount of low cost off the shelf opto-mechanical componentry from Newport and Thorlabs. Combining the above mentioned alignment tools with precision linear rails, linear encoders, high precision tooling balls, and alignment prisms allowed the optical alignment to be well constrained and completed in a deterministic fashion. This paper will detail the step by step alignment process of each optical element while including the equipment and design features used to make it an integrated process.

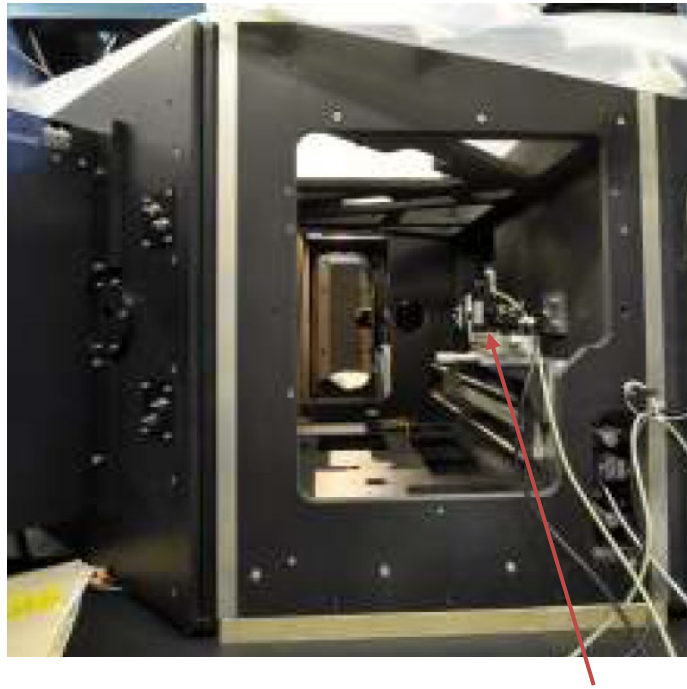


Figure 12: View looking down central spine during collimator alignment. PSM mounted on linear rail.

13) J. Brzeski, et. al., “Hermes – the engineering challenges”, Proc SPIE, 8446, 84464N (2012)

The design of the slit mask is presented in the Figure 12 and Figure 13. The high resolution slit is formed using two jaws per slitlet, top and bottom, to mask the image of the fibres produced by the slit relay lenses, thus forming the narrower slit. First the bottom jaw is adjusted in relation to corresponding v-groove with the help of a point source microscope (PSM) mounted on an XYZ optical coordinate measuring machine (see Figure 14). The bottom jaw adjustment pin is used to adjust the required position. The position of the top jaw is set by applying a 170  $\mu\text{m}$  shim between the top and bottom jaws and adjusting its location before securing it with M2 socket head cap screws. Both jaws are mounted to precise surfaces on the slit mask body which are perpendicular to v-groove axes. This approach and precision manufacturing of the slit mask body ensures that all slits are placed within required tolerance of the fibre image positions. The slit mask is attached to the slit with accuracy and repeatability of few micrometers by employing a kinematic mount system (see Figure 12). The slit mask is fixed to the slit by neodymium magnets installed on the slit LH and RH kinematic mount columns. Releasing the mask is accomplished by unscrewing the three mask release posts in close proximity to kinematic mounts (only one shown in Figure 12).

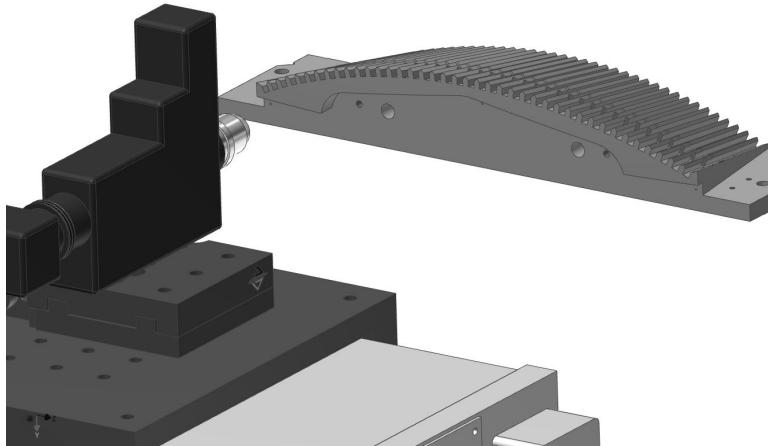


Figure 14. Mask alignment - step 1.

15) N. Staszak, et. al., "TAIPAN Fibre Feed and Spectrograph: Engineering Overview", Proc. SPIE, 9912, 991223 (2016)

The collimator and camera assemblies (Figure 21) are constructed of aluminum. They are designed to be aligned on the AAO lens centering station (LCS) with a Z stage mounted point source microscope (PSM) and an air bearing stage [7, 8]. Each lens is mounted in an individual cell, with the optical surface resting on a tangential cell surface. Lens cells are first run out on the precision AB Tech air bearing stage to form the opto-mechanical axis of the cell. The lens and cell are then rotated on the air bearing stage while the lens is tilted on the tangential seat. The return beam runout of the lens surfaces, as observed by the PSM, is minimized, thus bringing the optical axis of the lens to the established axis of the lens cell. An RTV bond is applied to the perimeter of the lens cell and an axial retention ring is threaded into place.

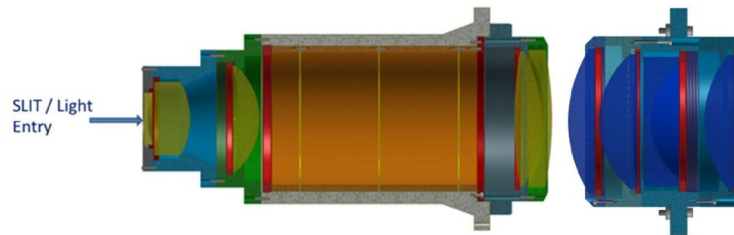


Figure 21. Cross Section of Collimator and Blue Camera.

20) R. Zhelem, et. al., "KOALA, a wide-field 1000 element integral-field unit for the Anglo-Australian Telescope: assembly and commissioning", Proc. SPIE, 147, 91473K, (2017)

The alignment setup for microlens arrays is based on the precision 3 axis stage. The stage carries a point source microscope (PSM) tool<sup>6</sup> looking down on the microlens arrays. The hexagonal microlens housing is shown in Fig. 4. The microlens array is bonded to the cell, then centred optically with respect to the pupil array and fixed to the housing using RTV. The point source microscope enables direct viewing of a fibre core through a pupil microlens as well as the referencing of fiducial points of microlenses in both arrays. Separation between arrays is controlled simultaneously with lateral positioning, it is set to the optimised prescription value to within 10  $\mu\text{m}$ .

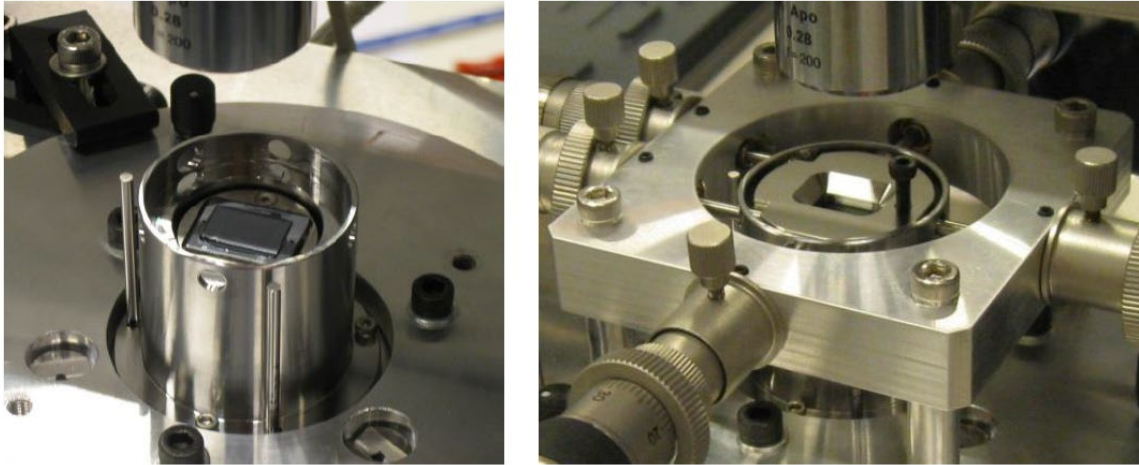


Figure 4. Pupil microlens array bonded to the IFU (left). Assembly of the hexagonal microlens array (right)

19) D. Brousseau, et. al., "SITELE optical design, assembly, and testing", Proc SPIE, 9147, 91473Z (2014)

The process is repeated in the second step of the tests where, this time, the interferometer is placed in front of the entrance of the camera optics (see Fig. 4) and both the BFL and PSF are again measured using the PSM mounted to an Aerotech ABL1000 air-bearing direct-drive linear stage.

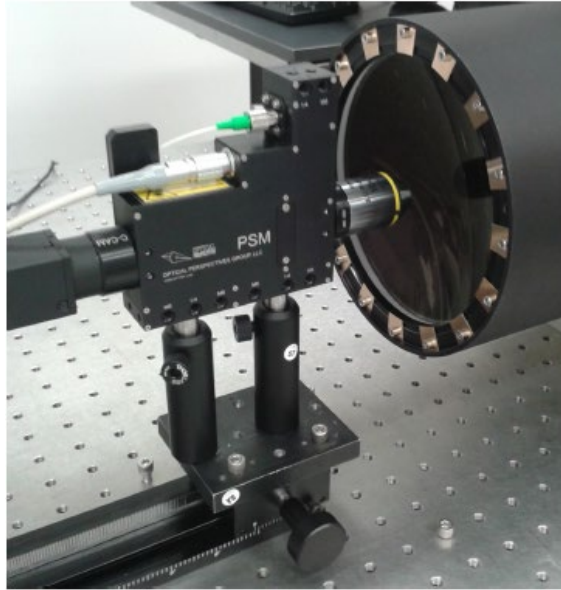


Fig. 5. Photograph of the PSM setup used to measure the BFL and the PSF of SITELE collimator.

18) Xin-Yin Jia, et. al., "Comprehensive design analysis and verification of space-based short-wave infrared coded spectrometer via curved prism dispersion," *Appl Opt*, 61(8), 2125 (2022)

The optical elements of the SSICS-CPD were composed of seven off-axis optical elements and one coding board. Taking the optical axis of any optical element as a reference, the optical axis of the other seven optical elements had a certain deflection angle with the reference optical axis, and the deflection angles were inconsistent. To realize high-precision and rapid assembly of the off-axis optical system, both the PSM and the CMM were used in this project. The PSM is a small package ( $\sim 100 \times 150 \times 30$  mm), including a point source of light, a beam splitter, a microscope objective, and a digital CCD camera to detect reflected light spot. The PSM adopts the principle of spherical autocollimation. When the point light source is located at the curvature center of the spherical mirror, the image point formed after reflection is also located at the curvature center of the spherical mirror. A software package, in conjunction with a computer video display, locates the return image in three degrees of freedom relative to an electronic spatial reference point



Fig. 19 Adjustment of the spatial position of each optical subassembly by the PSM on the CMM.



16) M. Wolf, et. al., Laboratory performance and commissioning status of the SALT NIR integral field spectrograph, Proc. SPIE, 12184, 1218407 (2022)

Before the NIR fiber cable was installed on the telescope, the SALT FIF was brought down to a laboratory bench and set up for calibrating the IFU positions in it using a point source microscope (PSM). The IFU and sky bundle were mounted into the FIF jaws, which is pictured in the center panel of Figure 21. The science IFU is in the left jaw and the sky bundle is in the right jaw. The PSM laser spot was set up on a reference pixel in the acquisition camera located at the top of the FIF (left panel of Figure 21) and the PSM was focused. The FIF was then translated to each fiber bundle, which was mechanically adjusted to make the polished fiber face parfocal with the FIF acquisition camera. After homing the FIF axes, they were translated to put the PSM spot onto corner fibers of each rectangular fiber array, recording the encoder positions of each corner. These measurements were used to calculate the encoder coordinates of a central fiber in the IFU for setting up on targets after they are acquired with the onboard camera and centered on its reference pixel.

The performance of the cam bars designed into the IFU mounts that angle the bundles telecentrically with jaw separation was also tested with the PSM. The spot was focused on the bundle surface with jaws at the minimum separation. The jaws were then moved to maximum separation and the PSM was translated to bring the spot into focus. The required focus translation distance, measured with a digital dial indicator, was compared to that required in the CAD model for the desired angle change. The distances matched.

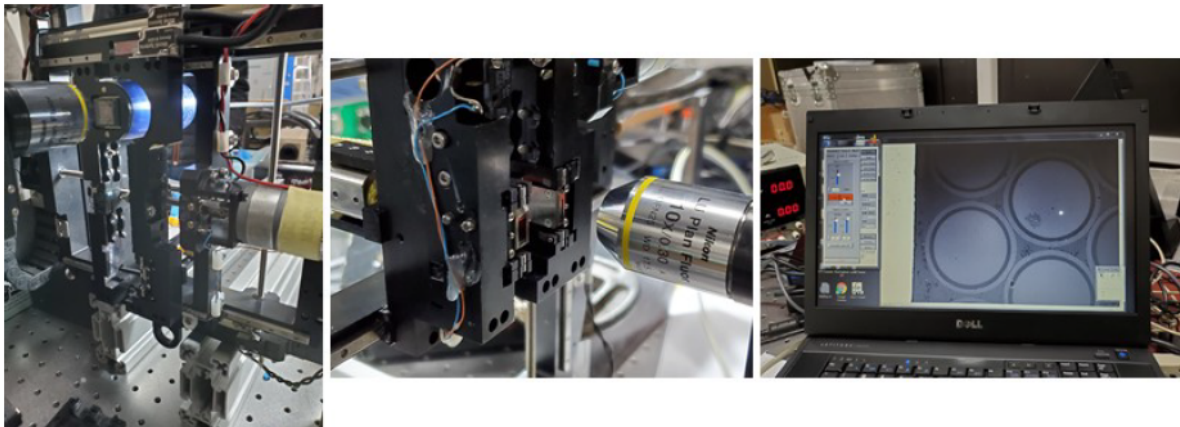


Figure 21. Calibration of the IFU positions in the fiber instrument feed. A point source microscope (PSM) was first set up on the reference pixel in the FIF acquisition camera (left). The microscope objective in the left and center panels is part of the PSM producing a red laser spot on the surface. FIF axes were then translated to position the PSM spot onto corner fibers of the IFU and sky bundle mounted in the jaws at the bottom of the FIF (center). The right panel shows the PSM spot on a 300-micron core fiber as a corner fiber was being moved toward it.

17) J. Brink, et. al. Preparing the SALT for near-infrared observations, Proc SPIE, 12182, 121822E (2022)

The Fiber Instrument Feed (FIF) forms the interface between the telescope focal plane and its fiber-fed instruments. The fiber positioning mechanism allows translation in two dimensions to position the selected fiber-pair near the optical axis and a separation stage to set the distance between the object and sky fibers. The Object “jaw” of the mechanism also includes an integral acquisition camera that is accurately calibrated to the location of each fiber pair. During operation the acquisition process involves centering the object in the acquisition camera and then using the FIF translation stages to “swap out” the camera for the selected object fiber. The separation stage with Object and Sky “jaws” is shown in Figure 11 (left). Laboratory calibration of the fiber locations with respect to the acquisition camera was performed using a Point-Source Microscope (PSM) from Optical Perspectives<sup>†</sup> (Figure 11, right). In preparation for integrating the SALT-NIR an off-the-shelf coherent fiber bundle from SCHOTT<sup>‡</sup> was installed on the Object “jaw” and its location and focus also mapped to the acquisition camera. This “test IFU” was used to mature the process of acquiring targets on a fiber bundle before the final science bundle was installed.

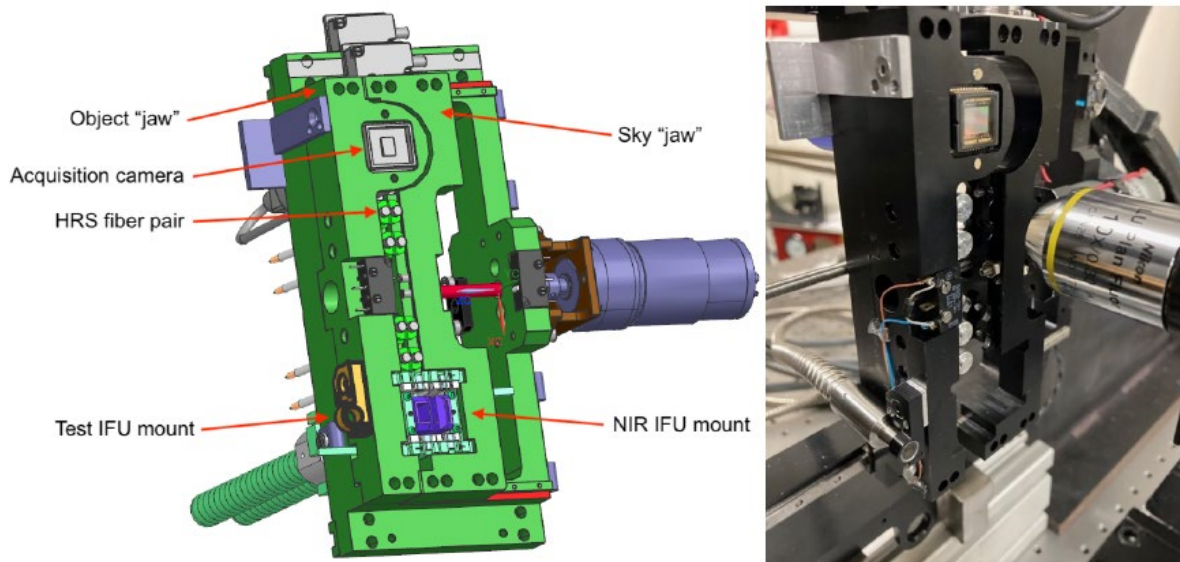


Figure 11. Left: Model of the Fiber Instrument Feed indicating acquisition camera, SALT HRS fibers and SALT-NIR IFUs. Right: Physical system during calibration using test fiber ferrules to simulate the location of the HRS fiber focal plane.

21) J. Zhu and W. Shen, Design and manufacture of compact long-slit spectrometer for hyperspectral remote sensing, *Optik* 247, 167896 (2021)

Fig. 8(a) and (b) are respectively an optical lay out and an axial view of the VNIR spectrometer. Folding mirrors are added in object space and image space for further reduction of volume. It is planar symmetrical and its slit length is 61.44 mm. Spectral sampling of this spectrometer is 0.83 nm for each pixel, and its spectral resolution is 5 nm when the detector is 6 binning at spectral dimension. According to the data in Table 1, off-axis magnitude of its slit is 0.55, and structural factors  $k_1' = 2.13$ ,  $k_2' = 0.82$ . Its imaging quality is close to the diffraction limit with negligible smile and keystone distortions, and its maximal RMS diameter of spot diagram is 6  $\mu\text{m}$ . Furthermore, the designed spectrometer has compact structure and high concentricity, which allows convenient alignment by using the Point Source Microscope [19].

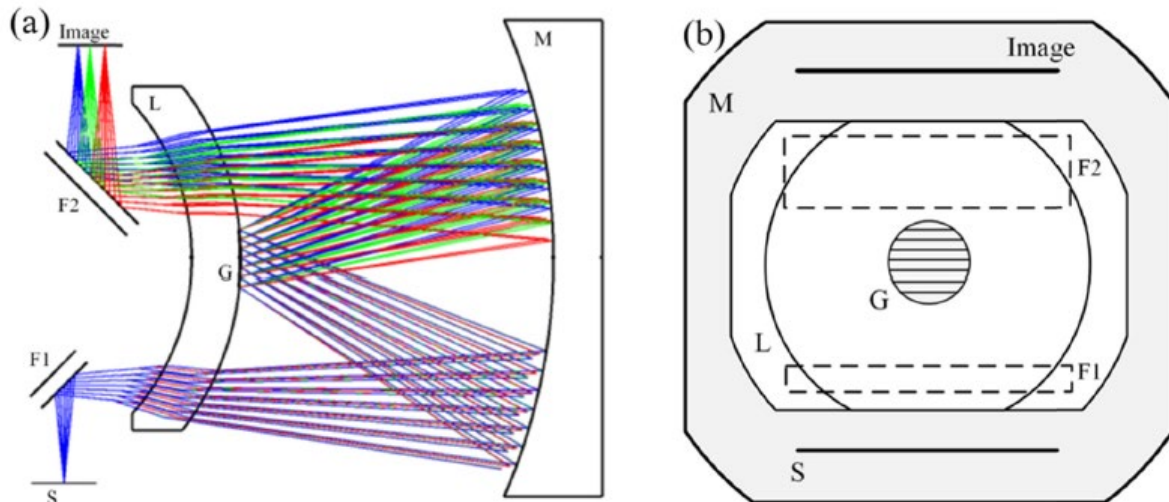


Fig. 8. (a) The designed VNIR spectrometers and (b) its axial view.

22) T. Chabot, et. al., GIRMOS image slicer: preliminary optical design, Proc. SPIE, 12184, 121845K (2022)

Using equipment at AOFI, we have been able to estimate the relative angle between two slices to  $(1.8 \pm 0.5)^\circ$ , which is close to the nominal  $1.87^\circ$ . After the finishing phase, absolute slice angles will be determined using a motorized goniometer and a point source microscope (PSM), by measuring the retroreflection. As for surface roughness, the narrow aperture implies that neither a profilometer nor an AFM could be used for metrology, so custom setups will need to be used in the future for that matter. Still, simulations and previous tests on RSA-6061 have shown that achieving the  $R_q \leq 7.5$  nm requirement should be feasible given the correct parameters.<sup>5</sup>

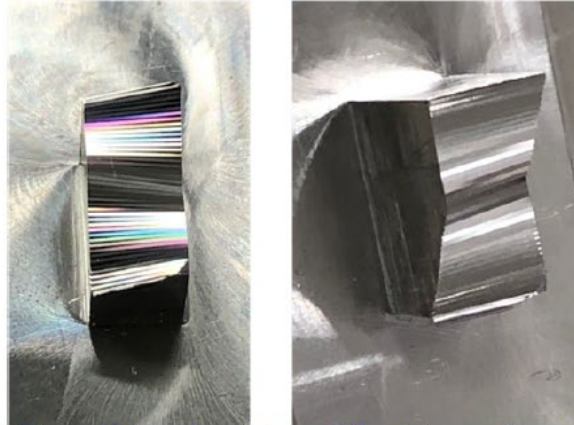


Figure 15: Diamond-turned prototype of the staircase slicer stack design.

24) S. Kanodia, et. al., Overview of the spectrometer optical fiber feed for the Habitable-zone Planet Finder, Proc. SPIE, 10702, 107026Q (2018)

We installed our point source microscope (PSM) with a Thorlabs telecentric lens on top of the fiberhead to document the process and verify concentricity. The telecentric lens gives a large field of view. Figure 8 shows the setup. Post gluing the lens we used a Teflon weight to hold down the lens as the epoxy was left to dry over 2 days.



(a) Microscope setup to image the fiberhead during gluing.



(b) RG695 lens glued on top.

Figure 8: Gluing of the RG695 lens on the fiberhead

30) F. Xihong, Research on Precision Measurement and Assembly Technology of Fery Prism, Proc. SPIE, 11763, 1176304 (2021)

Based on the special structure of curved surface prism, its processing technology and its function in Spectral Imager, an assembly inspection platform based on a high-precision CMM, a point-source microscope (PSM) and a high-precision rotary device is established, as shown in Fig.5, based on the principle of space measurement, the principle of point source collimation and the three-dimensional mathematical modeling, the Assembly and alignment of Fery prism are studied.

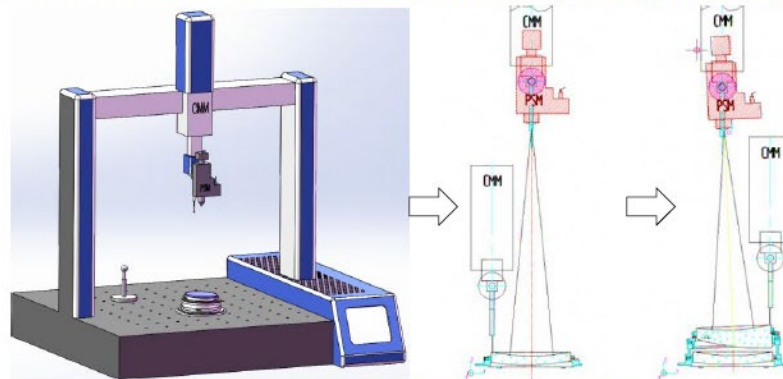


Fig.5 Assembly Process Method of Curved Prism